ChemComm

RSC Publishing

COMMUNICATION

View Article Online
View Journal | View Issue

Direct object resolution by image subtraction: a new molecular ruler for nanometric measurements on complexed fluorophores†

Cite this: *Chem. Commun.*, 2013, **49**, 5559

Received 21st March 2013,
Accepted 2nd May 2013

DOI: 10.1039/c3cc42072h

www.rsc.org/chemcomm

Rémi L. Boulineau and Mark A. Osborne*

A technique for measuring distances between two or more fluorophores spaced in the 10–100 nm range is described. We identify a linear correlation between the intensity–amplitude in the difference-image of single molecules undergoing fluorescence fluctuations and their separation. The transform is used to map distances between coupled fluorophores.

Super-resolution techniques are now providing information on subcellular structures and biological mechanism at spatial scales, previously inaccessible with conventional microscopy.[1–5] While resolutions of 20 nm or less (FIONA)[6] can readily be achieved, experiments can be complex, either in instrumentation or in post-acquisition image analysis and point-spread-function (PSF) fitting. On the other hand, super-resolution optical fluctuation imaging (SOFI)[7] is elegant in its simplicity, based only on the high-order analysis of temporal fluctuations in single molecule fluorescence. However, for emitters only a few tens of nanometers apart, SOFI cannot readily separate the contributions from individual fluorophores. Alternative techniques exploit photobleaching,[8,9] blinking,[10–12] transient adsorption[13] or spectral differences[14] of multiple fluorophores in close proximity to retrieve individual localisations *via* conventional PSF-fitting.

Here we present a novel way to measure the distance between molecular centres directly from information in the difference-image of independently fluctuating single molecules. Specifically, we show a simple linear transform exists between the central intensity gradient in the difference-image of two closely spaced PSFs and their separation. The intrinsic fluorescence intermittency of quantum dots (QDs), coupled to the ends of a 100 bp double-stranded dsDNA (34 nm) in a dimeric complex is used to demonstrate the principle of direct object resolution by image subtraction (DORIS) and application of the technique to a higher order QD multimer highlights the generic nature of the approach. We demonstrate how DORIS can readily distinguish multimeric structures from single QDs and that measurement of the distance between fluorophores separated on the 10–100 nm scale is quantitative.

To illustrate the concept, consider two point emitters separated by a distance much less than the Rayleigh limit, 0.61λ/NA, for the resolution of their PSFs. Below this limit the PSFs strongly overlap such that emission typically appears to arise from a single source. However, subtraction of the individual PSFs from each other results in a difference-image that contains intensity maxima and minima at locations that are weakly related to, but well separated from, the emitting centres. More significant is the intensity-gradient between the extrema in the difference-image which is strongly correlated with the separation of the PSF centres. The correlation is most clearly highlighted in the difference between the 1D PSF cross-sections of two molecules separated at increasing distances (Fig. 1a). On the other hand, the position of the maxima and minima in the difference curve, appear far less sensitive to PSF displacement. For simulations of closely spaced PSFs in 2D (S1, ESI†), the sum image is

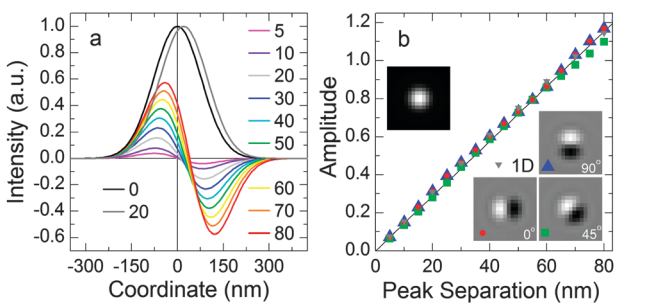

Fig. 1 Direct object resolution by image subtraction. (a) Normalised 1D PSF cross-sections centred at the origin (black) and 20 nm along x (gray). The difference between PSFs (light gray) at 20 nm separation is shown along with difference curves for PSF-separations of 5 to 80 nm showing distance dependent gradients. Here, the Gaussian function $I(x) = \exp(-(x - x_0)^2/2s^2)$ with standard deviation $s = \lambda/4\mathrm{NA}\sqrt{2\ln 2}$, λ = 530 nm and NA = 1.45, is used to represent the PSF cross-section. (b) DORIS amplitude-to-separation conversion curves. Amplitudes are derived from the difference between intensity maxima and minima in the difference-images of two simulated PSFs displaced along a vector at 0°, 45° and 90° to the x-ordinate. Difference-amplitudes from the 1D-Gaussians are also shown along with a linear-fit for guidance.

Department of Chemistry, School of Life Sciences, University of Sussex, Falmer, BN1 9QJ, UK. E-mail: m.osborne@sussex.ac.uk; Fax: +44 (0)1273 78323; Tel: +44 (0)1273 678328

† Electronic supplementary information (ESI) available: Experimental procedure and image analysis, simulation details and analysis of localisation and distance uncertainties. See DOI: 10.1039/c3cc42072h

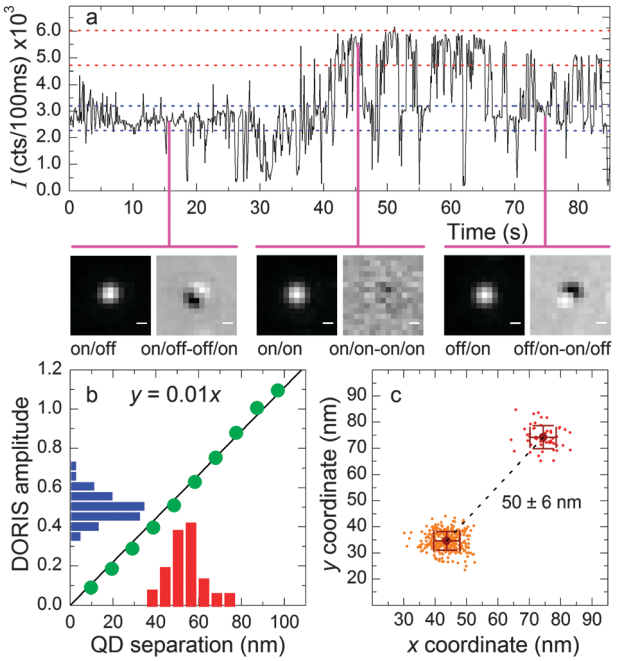

Fig. 2 Direct resolution of a dsDNA-QD dimer by image subtraction. (a) Integrated fluorescence intensity trajectory of a typical diffraction-limited dimer with images of QDs in on/off [10], on/on [11] and off/on [01] states and corresponding difference-images [1−1], [00] and [−11]. Scale bar 200 nm. (b) DORIS amplitude-to-separation conversion curve (green points) for the experimental resolution, 97 nm per pixel at 165× magnification and 2 × 2 pixel averaging of intensity maxima and minima in the difference-image. Also shown are the histograms of difference-amplitudes (blue) centred at 0.51 ± 0.06 and corresponding QD distances (red) centred at 53 ± 6 nm. (c) Localisations of the two QD centres in the dimer from conventional Gaussian fitting showing QD separation is in good agreement with the DORIS derived distance.

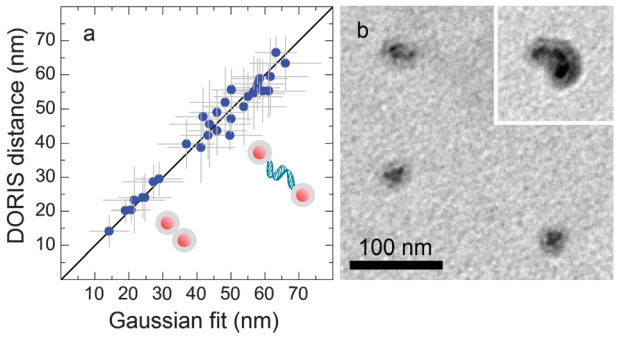

Fig. 3 Correlation plot between couple-QD separations derived from DORIS and distances from single molecule localisations in 30 QD-dimers. Uncertainties in both measurements are determined from the analysis of multiple frames from the image stack of each QD-dimer. A straight line representing the one-to-one correspondence is plotted for guidance. (b) TEM image of individual 585 nm streptavidin functionalised QDs with average core–shell diameter 23 ± 4 nm and (inset) a non-specifically coupled cluster of three QDs showing centre-to-centre distance of approx. 21 nm is not strongly influenced by surface functionality.

largely indistinguishable from the image of a single PSF (Fig. 1b, inset), while image subtraction reveals the same differential structure (in profile) as the 1D cross-section. Intensity variation in the difference-image contains information on the position of each molecule with respect to each other. Here, we exploit the sensitivity of the gradient in the difference-image with respect to PSF separation to generate a linear amplitude-to-distance correlation curve from which distances between molecules can be read directly (Fig. 1b). For simplicity the difference-amplitude rather than gradient is used, since the distance between intensity maxima and minima is insensitive to PSF separation. We find the difference-amplitude for both the 1D PSF cross-sections (Fig. 1a) and 2D PSF simulations show near-identical linear dependences on PSF separation. A small deviation in the correlation curve for 2D PSFs displaced along a vector oriented 45° to the x or y axes, arises from finite pixel size effects, but with an error of less than 10 nm at 80 nm displacement, the amplitude-to-separation conversion curves appear universal and largely independent of the direction of PSF displacement.

In a proof-of-application, we have used DORIS on closely coupled-QDs, where blinking in the fluorescence of at least one QD will result in a shift in centre-of-mass of the PSF and hence well-resolved difference-images. Streptavidin functionalised QDs (M10111P, Life Technologies) were coupled using 100 bp complementary sequences of biotinylated DNA (S2, ESI†) deposited on glass coverslips and imaged using total internal reflection fluorescence (TIRF) microscopy with typical capture rates of 10 fps into stacks of up to 2500 frames. The simplest approach to analyzing the image set of n frames $A = \{1\ldots n\}$, is to generate the set of difference-images, $B = \{1\ldots n(n-1)/2\}$, where each frame $B_{ij} = A_i - A_j$ for all i and $j > i$. In this case, two coupled-QDs independently switching between *on*(1) and *off*(0)-states generate on/off [10] and off/on [01] frame combinations that give rise to difference images [1−1] and [−11] with amplitudes between intensity extrema that are dependent on both QD separation and absolute intensities. Here, we introduced a binary notation to represent the state of each QD in an image frame [ ] and the result of image subtraction for simplicity. Normalizing QD peaks in each image prior to subtraction removes the intensity dependence, allowing QD distances to be read directly using the linear amplitude-to-separation transform.

In general, from the fluorescence trajectory of two QDs in close proximity (Fig. 2a), the [11] state (both QDs on) can be easily identified from the two level intensity trajectory. However, differentiating [10] from [01] states is only made clear through difference-imaging. Difference-images corresponding to [10] − [01] = [1−1], [11] − [11] = [00] and [01] − [10] = [−11] exemplify the DORIS process. Note that image stacks were corrected for stage-drift prior to image subtraction, a process essential to achieving image alignment and reduced uncertainty in localisation and distance measurements (S3, ESI†). Intensity–amplitudes in the difference-images of type [1−1] and [−11], are mapped directly to QD separation using the amplitude-to-separation curve (Fig. 2b green points). The histogram of amplitudes derived from the DORIS analysis across the image stack with mean amplitude 0.51 ± 0.06 (Fig. 2b blue bars) converts to a distribution of distances with mean QD separation of 53 ± 6 nm (Fig. 2b red columns).

We compared QD separations derived from amplitude-to-distance conversion with separations measured between single molecule localisations. DORIS was first used to differentiate [10] frames from [01] frames before locating each QD across all frames in each image set by fitting the 2D Gaussian function $I(x,y) = \exp[-(x - x_{1(2)})^2/2s^2 - (y - y_{1(2)})^2/2s^2] + I_0$ to the PSF of QD 1 and (2) separately (Fig. 2c). QD separations were then determined from the vectorial distance $[(x_1 - x_2)^2 + (y_1 - y_2)^2]^{1/2}$. Uncertainties of $\sigma \pm 7$ nm in the localisation coordinates result

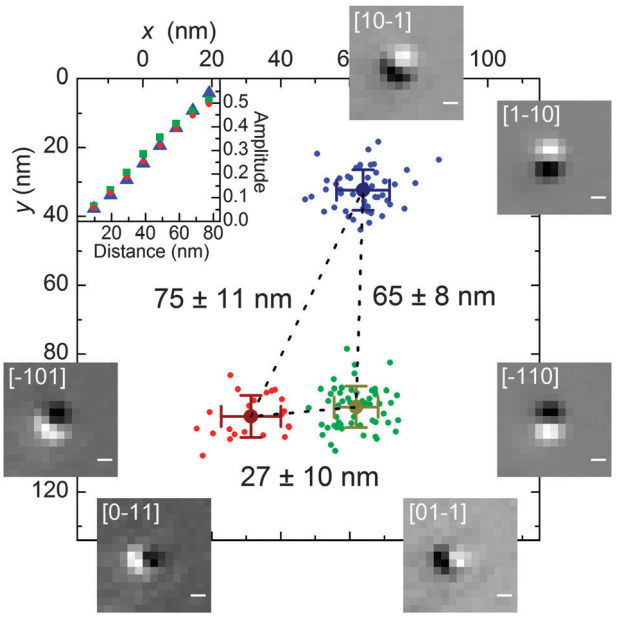

Fig. 4 Resolution of a sub-diffraction limited QD-multimer by DORIS. Single-QD localisations *via* Gaussian-fitting to individual PSFs are shown (red, green, blue) with distances determined from a DORIS analysis of intensity–amplitudes in the set of difference-images (subset shown overlaid). DORIS derived distances in the figure correspond closely to centre-of-mass separations from the individual QD localisations 63.0 ± 8.4 nm (blue-green), 30.6 ± 10.7 (green-red) and 73.2 ± 9.2 (red-blue). Difference-images are shown for the various combinations of pair-wise subtractions of frames in which one QD is on(1) and the others are off(0): blue = [100], green = [010] and red = [001]. Scale bar is 200 nm. (Inset) Amplitude-to-distance conversion curves along the QD displacement vectors (blue triangle = blue-to-green, green square = green-to-red, red circle = red-to-blue).

primarily from stage-drift, but also photon counting (Fig. S4 in ESI†) and ultimately propagate to an error of about ±10 nm in the distance between QDs. We find excellent one-to-one correspondence between DORIS derived distances and those measured by conventional localisation (Fig. 3a) across the population of QD-dimers analyzed. The result supports DORIS as a quantitative method of determining fluorophore separation in sub-diffraction limited nanostructures and complexes. The analysis reveals two populations of dimeric QD structures with different separations. We attribute a population emergent with distances centred at 23 ± 6 nm to directly and non-specifically coupled QDs. The value is consistent with the mean diameter, 23 ± 4 nm for individual streptavidin functionalised 585 nm QDs and centre-to-centre distances in QD clusters measured under TEM (Fig. 3b). A larger population of QDs found at 52 ± 11 nm separation is attributed to dsDNA coupled dimers, a value consistent within error of the QD diameter and an extended 100 bp DNA length of 34 nm.

In a further demonstration of DORIS, we extended difference-imaging to a trimeric-QD complex. Given the functionality of the QD extends over its entire surface and the tetravalent nature of the streptavidin binding protein, multiple DNA binding and formation of multimeric QD structures is expected. A DORIS analysis of the trimeric QD cluster in this case reveals all difference-images derived from combinations of the individual QD *on*-state frames [100], [010], [001] (Fig. 4). Respective QD separations 65.4 ± 8.1 nm, 26.5 ± 10.3 and 74.6 ± 11.4 determined from intensity amplitude-to-distance conversion in the difference-image combinations [1−10], [01−1] and [10−1] again show excellent agreement with the corresponding vectorial distances between Gaussian-localised QDs, 63.0 ± 8.4 nm, 30.6 ± 10.7 nm and 73.2 ± 9.2 nm. In this case, the QD-trimer appears to be constructed of two DNA-coupled QDs (50–60 nm) with a third QD coupled either non-specifically (20–30 nm) or with significantly compressed dsDNA.

We have developed DORIS as a novel method for resolving closely spaced fluorophores, with separations well below the diffraction-limit. Applied to multimeric-QD structures, we have shown that distances derived using DORIS are quantitative (within error) with respect to those calculated by conventional localisation techniques and consistent with TEM measurements. We note that in principle DORIS only requires modulation in the fluorescence with sufficient depth to produce intensity variation in the difference-image (S5, ESI†). For this purpose, fluorescence flickering in organic dyes, switching in fluorescent proteins could be utilized.[15,16] We envisage the method as complimenting established super-resolution techniques of PALM, STORM, SOFI and their derivatives, where high labeling densities or non-specific interactions can prohibit unambiguous resolution of fluorophores by conventional PSF fitting. Alternatively, we expect DORIS will find application in molecular counting in protein–protein(DNA) interactions and higher-order assembly of biological structures and offers the potential to provide structural information from the direct measurement of molecular separations.

We acknowledge the EC (FP7 grant 215148) for supporting R.B. and Prof. A. M. Carr and Dr A.-S. Schruers for their useful comments. We also thank Ms H. Aitchison (Nuffield Foundation undergraduate bursary) for help with aspects of image processing.

Notes and references

1 S. W. Hell and J. Wichmann, *Opt. Lett.*, 1994, **19**, 780–782.
2 M. G. L. Gustafsson, *J. Microsc.*, 2000, **198**, 82–87.
3 E. Betzig, G. H. Patterson, R. Sougrat, O. W. Lindwasser, S. Olenych, J. S. Bonifacino, M. W. Davidson, J. Lippincott-Schwartz and H. F. Hess, *Science*, 2006, **313**, 1642–1645.
4 S. T. Hess, T. P. K. Girirajan and M. D. Mason, *Biophys. J.*, 2006, **91**, 4258–4272.
5 M. J. Rust, M. Bates and X. Zhuang, *Nat. Methods*, 2006, **3**, 793–795.
6 A. Yildiz, J. N. Forkey, S. A. McKinney, T. Ha, Y. E. Goldman and P. R. Selvin, *Science*, 2003, **300**, 2061–2065.
7 T. Dertinger, R. Colyera, G. Iyer, S. Weiss and J. Enderlein, *Proc. Natl. Acad. Sci. U. S. A.*, 2009, **106**, 22287–22292.
8 M. P. Gordon, T. Ha and P. R. Selvin, *Proc. Natl. Acad. Sci. U. S. A.*, 2004, **101**, 6462–6465.
9 X. Qu, D. Wu, L. Mets and N. F. Scherer, *Proc. Natl. Acad. Sci. U. S. A.*, 2004, **101**, 11298–11303.
10 K. A. Lidke, B. Rieger, T. M. Jovin and R. Heintzmann, *Opt. Express*, 2005, **13**, 7052–7062.
11 B. C. Lagerholm, L. Averett, G. E. Weinreb, K. Jacobson and N. L. Thompson, *Biophys. J.*, 2006, **91**, 3050–3060.
12 D. T. Burnette, P. Sengupta, Y. H. Dai, J. Lippincott-Schwartz and B. Kachar, *Proc. Natl. Acad. Sci. U. S. A.*, 2011, **108**, 21081–21086.
13 P. D. Simonson, E. Rothenberg and P. R. Selvin, *Nano Lett.*, 2011, **11**, 5090–5096.
14 X. Shi, Z. Xie, Y. Song, Y. Tan, E. S. Yeung and H. Gai, *Anal. Chem.*, 2012, **84**, 1504–1509.
15 S. Habuchi, R. Ando, P. Dedecker, W. Verheijen, H. Mizuno, A. Miyawaki and J. Hofkens, *Proc. Natl. Acad. Sci. U. S. A.*, 2005, **102**, 9511–9516.
16 M. Heilemann, S. van de Linde, M. Schuttpelz, R. Kasper, B. Seefeldt, A. Mukherjee, P. Tinnefeld and M. Sauer, *Angew. Chem., Int. Ed.*, 2008, **47**, 6172–6176.